Exploring the S*n* Binding Pockets in Gingipains by Newly Developed Inhibitors: Structure-Based Design, Chemistry, and Activity

Arkadiusz Białas,[†] Jolanta Grembecka,[†] Daniel Krowarsch,[‡] Jacek Otlewski,[‡] Jan Potempa,[§] and Artur Mucha*[,†]

Department of Bioorganic Chemistry, Faculty of Chemistry, Wrocław University of Technology, Wybrzeże Wyspiańskiego 27, 50-370 Wrocław, Poland, Institute of Biochemistry and Molecular Biology, University of Wrocław, Tamka 2, 50-137 Wrocław, Poland, Department of Microbiology, Faculty of Biotechnology, Jagiellonian University, Gronostajowa 7, 30-387 Kraków, Poland, and Department of Biochemistry and Molecular Biology, University of Georgia, Athens, Georgia 20605

Received January 6, 2006

Arg-gingipains (Rgps) and Lys-gingipain (Kgp) are cysteine proteinases secreted by *Porphyromonas gingivalis*, the major pathogen implicated in periodontal disease. Gingipains are essential to the bacterium for its virulence and survival, and development of inhibitors targeting these proteins provides an approach to treat periodontal diseases. Here, we present the first example of structure-based design of gingipains inhibitors, with the use of the crystal structure of RgpB and the homology model of Kgp. Chloromethyl ketones were selected as suitable compounds to explore the specificity of the S*n* binding region of both enzymes. Three series of inhibitors bearing Arg or Lys at P1 and different substituents at P2 and P3 were designed, synthesized, and tested. High potency (k_{obs}/[I] $\sim 10^7$ M^{-1} s^{-1}) was achieved for small ligands, such as the dipeptide analogues. The detailed analysis of S*n* binding pockets revealed the molecular basis of inhibitory affinity and provided insight into the structure−activity relationship.

Introduction

Periodontitis represents a group of infectious oral diseases connected with chronic inflammation of the gingiva, destruction of the periodontal tissue, and alveolar resorption, eventually leading to exfoliation of teeth. Recently, an association between periodontal disease and certain pathological states, such as atherosclerosis and coronary heart diseases,[1,2] pneumonia,[3] diabetes,[4] multiple sclerosis,[5] preterm birth, and low birth weight,[6−8] has been demonstrated. *Porphyromonas gingivalis*, a Gram-negative anaerobic bacterium, has been recognized as the primary cause of some types of periodontitis, including chronic adult periodontitis.[9,10] This bacterium secretes high level of cysteine proteases, referred to as gingipains.[11,12] Gingipains degrade many proteins of human connective tissue and plasma, including immunoglobulins, proteinase inhibitors, and collagens. This process provides nutrients for the bacteria, making gingipains essential for growth and survival of the bacteria in the periodontal pockets. Furthermore, these enzymes play a crucial role in hemagglutination, coaggregation, hemoglobin binding, and acquisition of heme and amino acids from the host by the pathogen.[13,14] Gingipains also cause disruption to a number of highly controlled human pathways: kallikrein−kinin cascade, blood coagulation, and the host defense systems.[15−17] Endogenous protease inhibitors have little or no effect on the proteolytic activity of gingipains.[17,18] All of these findings indicate that regulation of gingipain's activity by appropriate inhibitors should have important biomedical implications.[8,19,20]

Gingipains exhibit the exquisite specificity for the cleavage of peptide bonds between either Arg-Xaa (arginine specific cysteine proteinases RgpA, HRgpA, RgpB) or Lys-Xaa (lysine specific cysteine proteinase, Kgp).[12,21−23] RgpA and RgpB are essentially identical at the *N*-terminal portion, which includes the catalytic domain (*N*-terminal 351 residues of RgpB), while the *C*-terminal segment shows significant divergence. Gingipains form a separate family of cysteine proteases, as they exhibit no sequence similarity to any other known proteins. These unique properties make them attractive targets for the rational design of new potent and selective inhibitors. Nonetheless, only several gingipain inhibitors have been reported so far.[20] These include natural polypeptides and proteins: histatin 5 from human saliva (inhibits RgpB and KgP) with broad specificity for inhibiting proteases;[24] baculovirus p35, a natural caspase inhibitor (inhibits Kgp);[25] and a single point mutant of cowpox viral cytokine-response modifier, CrmA (Asp>Lys), which inhibits Kgp.[25] Besides, a natural inhibitor, phenylalanyl-ureido-citrullinyl-valyl-cycloarginal (**15**, FA-70C1), isolated from *Streptomyces*,[26] as well as the antibiotics doxycycline and tetracycline[27] have been identified as RgpB inhibitors. Furthermore, a few synthetic inhibitors such as the (acyloxy)methyl ketone inhibitor Cbz-Phe-Lys-CH_2OCO-2,4,6-Me_3Ph (inhibits Kgp);[28] peptidyl chloromethyl ketones (inhibit RgpB and Kgp);[28] ketopeptides Cbz-Lys-Arg-CO-Lys-N(CH_3)$_2$ (**16**, KYT-1, RgpB inhibitor), Cbz-Glu(NHN(CH_3)Ph)-Lys-CONHCH_2Ph (**17**, KYT-36, Kgp inhibitor),[8] and 1-(3-phenylpropionyl)piperidine-3(*R*,*S*)-carboxylic acid [4-amino-1(*S*)-(benzothiazole-2-carbonyl)butyl]amide (**18**, A71561, Kgp inhibitor);[29] aza-peptide Michael acceptors (Kgp inhibitors);[30] and benzamidine inhibitors (targeting RgpB)[31] have been reported (for structures **15**−**18**, see Figure 6). The majority of these compounds do not represent low molecular weight inhibitors and were either isolated from natural sources or synthesized on the basis of enzyme substrates. In this context, a rational design with the use of the protein structure constitutes a novel approach toward development of gingipain's ligands containing substituents that do not represent natural amino acids. Such inhibitors should fit tightly to the enzyme binding pockets, ensuring the increased binding affinity and selectivity versus other cysteine proteases.

The most effective strategy in construction of inhibitors for cysteine proteases is synthesis of compounds bearing a moiety able to bind covalently to the thiol residue in the active site.[32,33] Among them, chloromethyl ketones represent an interesting class of potent, irreversible alkylating agents. Although very reactive versus various nucleophiles and therefore relatively easy to inactivate under physiological conditions, they seem to be

* Corresponding author. Tel: +48−71−320−3354. Fax: +48−71−328−4064. E-mail: artur.mucha@pwr.wroc.pl.
[†] Wrocław University of Technology.
[‡] University of Wrocław.
[§] Jagiellonian University and University of Georgia.

10.1021/jm0600141 CCC: $33.50
Published on Web 02/10/2006

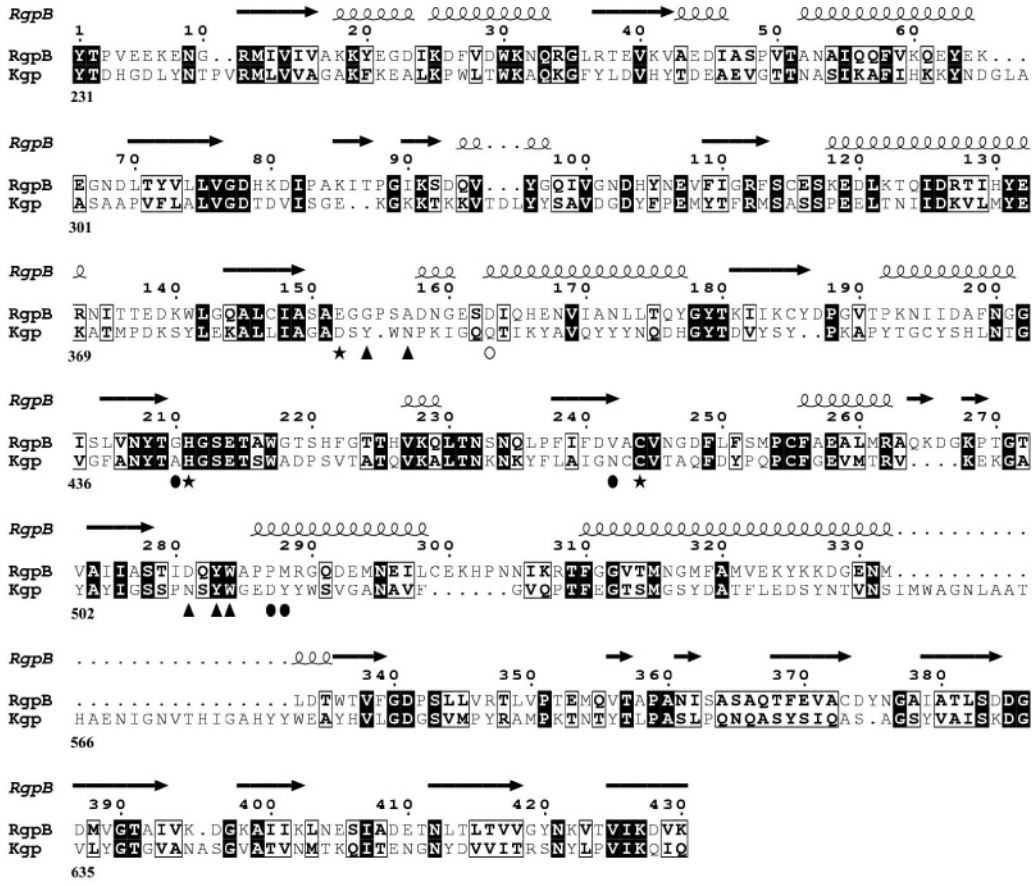

Figure 1. Sequence alignment of Kgp (gi number 1314751) with RgpB (sequence subtracted from PDB file 1CVR) obtained with ClustalW program. Figure prepared using the ESPript program (http://prodes.toulouse.inra.fr/ESPript/). Secondary structures of RgpB: helices (shown as springs), β-sheets (presented as arrows), and 3_{10} helices (indicated as smaller springs), are plot on the top of the alignment. Amino acids conserved in both gingipains are white and shown in black boxes, while similar amino acid (similarity defined by default parameters in ESPript) are black and shown in white boxes. Numbering of RgpB sequence is shown on the top of the alignment; Kgp amino acids are numbered on the bottom of the alignment. Amino acids forming the catalytic triad in Kgp and RgpB are indicated by black stars; black triangles point out the residues of the S2 and S3 pockets in both gingipains; black circles show Kgp residues involved in the formation of S1 pocket; the white circle indicates D163 in RgpB engaged in the salt bridge/hydrogen bond with Arg at P1 of the inhibitors.

suitable model compounds to exploit the binding preferences of gingipains.

In this paper, we present the application of structure-based ligand design strategy to develop new inhibitors of RgpB and Kgp, on the basis of the X-ray structure of RgpB. Since the Kgp structure is unknown, a 3D model of this protein based on the sequence similarity to RgpB was built. Subsequently, the computer program LUDI/Insight II[34,35] was employed for designing new gingipain ligands to exploit the S2 and S3 pockets of RgpB and KgP (definition of the S*n* and S*n*′ binding pockets in proteases as well as the P*n* and P*n*′ side chains of protease substrates and inhibitors is based on commonly used terminology introduced by Schechter and Berger[36]). This resulted in three series of chloromethyl ketones bearing Lys or Arg at P1 and different substituents at the P2 and P3 positions. The details of their design, synthesis, and binding affinities toward the enzymes are presented and discussed. The effectiveness of the tested inhibitors is analyzed in the context of their potential interactions with both gingipains. The corresponding S*n* binding pockets are compared, revealing the molecular basis for their substrate specificity and providing insight into the structure−activity relationship of gingipain ligands. The selected substituents will serve as important structural elements in preparation of less reactive and more selective gingipain inhibitors.

Results and Discussion

Homology Model of Kgp and Molecular Basis of Gingipain Substrate Specificity. The catalytic domain of Kgp (residues 231−698) exhibits about 26% overall sequence identity and 40% sequence similarity to the catalytic domain of RgpB. Since RgpB is the only protein with a known 3D structure homologous to Kgp, it served as a template to build the 3D model of the latter. The sequence alignment was prepared using the ClustalW program, with a few manual corrections (Figure 1). The residues forming the catalytic triad in Kgp—Cys477, His444, and Asp388—are placed at the positions corresponding to the analogous residues in RgpB—Cys244, His211, and Glu152 (Figures 1 and 2A). Interestingly, the sequence alignment reveals significant divergence in terms of the amino acid composition and their location in both sequences for the S1 pocket residues (Figure 1 and 2B,C) and relatively high similarity for the S2 and S3 binding regions (Figures 1 and 2D).

The sequence alignment served to build the model of the catalytic domain of Kgp, by employing the Modeller program.[37] Analysis of the obtained model and the crystal structure of RgpB complexed with D-Phe-Phe-Arg-CH_2Cl (FFR-CH_2Cl)[38] evidenced the differences in the S1 pocket architecture of both proteases, ensuring their distinct substrate specificity. The residues forming the S1 pocket in Kgp make favorable interac-

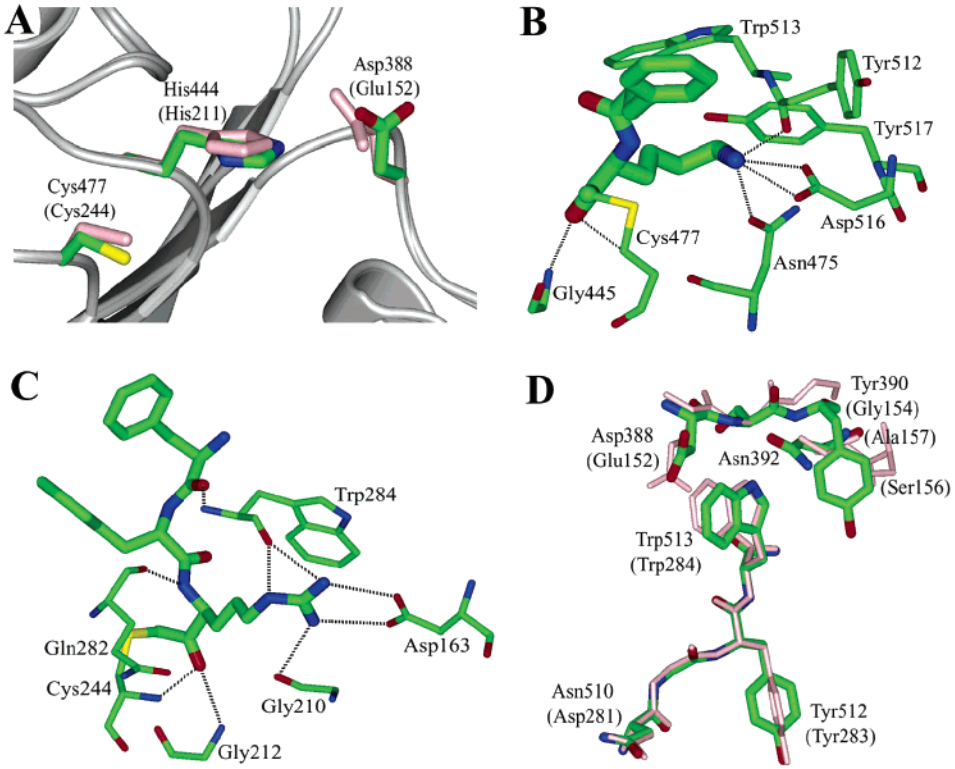

Figure 2. Active site and binding pockets in gingipains. (A) Catalytic triad in Kgp (colored according to atom types: C, green; N, blue; O, red; S, yellow) and RgpB (pink), originating from the superimposed model of Kgp onto RgpB structure. Numbering of RgpB amino acids is shown in parentheses. (B) Interactions of the S1 pocket of Kgp (residues shown as thin sticks) with Lys at P1 of the inhibitor **1a** (thick sticks). (C) Interaction mode of FFR-CH_2Cl (thick sticks) with RgpB (thin sticks), with coordinates taken from 1CVR. Residues of the S2 pocket are not shown for clarity of the figure. (D) Superimposed S2 and S3 pockets of Kgp onto the corresponding pockets of RgpB (coloring and numbering as in part A).

tions with the P1 Lys side chain (Figure 2B), which is characteristic for natural substrates of the enzyme. Both the salt bridge/hydrogen bond network with Asp516, Tyr512, Trp513, and Asn475, together with the hydrophobic interactions with Trp513, Tyr517, and Ala443, make Lys the optimal substituent at the P1 position of Kgp ligands. Although the side chain of Arg fits into the S1 pocket of Kgp, the interaction mode is not so favorable (reduced number of hydrogen bonds, data not shown). The salt bridge between the guanidine of P1 Arg and the carboxylate of Asp516 as well as the hydrophobic interactions with Trp513 of Kgp are the major possible contacts. This finding can explain the 20−50-fold decreased affinity of ligands bearing Arg in comparison to the optimal Lys at P1, when tested against Kgp.[28]

The specificity of RgpB toward Arg at P1 of a ligand is much more restricted. The guanidine group located in close proximity to the carboxylate of Asp163 forms the corresponding 2N−2O salt bridge (Figure 2C). In addition, it is involved in three hydrogen bonds with carbonyl groups of Trp284 and Gly210. Such interactions in a specific narrow S1 pocket covered by a lid formed by the Trp284 side chain are strictly discriminating against residues other than arginine. Although the side chain of lysine can be accommodated in the S1 pocket of RgpB, the salt bridge with Asp163 and hydrophobic contacts are the only possible interactions (data not shown). Such high preference was verified by observing a decrease in the inhibition rate constant of up to 3 orders of a magnitude for inhibitors bearing different amino acids, including Lys versus Arg at P1, tested toward RgpB.[28]

The S2 pockets in Kgp and RgpB are similar to each other. Asn510 and Tyr512 are involved in formation of this pocket in Kgp, which remains open to the solvent (Figure 2D). The spatial arrangement of these two residues is expected to be analogous to the corresponding Asp281 and Tyr283 in RgpB. However, the orientation of the side chain amide group of Asn510 remains ambiguous. In our structure-based design studies, we kept the oxygen atom of the Asn510 amide oriented toward P2 of the ligand. This retained the hydrogen-bond-acceptor group as a part of the S2 pocket similar to RgpB. However, its reverse location cannot be excluded, since this amide is not involved in any intramolecular hydrogen bond.

The S3 binding pockets in both gingipains are open to the solvent (Figure 2D). However, in Kgp the S3 pocket is somewhat deeper than the corresponding one in RgpB. The side chains of Trp513, Asp388, Tyr390, and Asn392, together with the backbone of 388−390 residues, are involved in its formation. The residues Trp284, Glu152, Gly154, Ala157, and Ser156, as well as the backbone of 152−154 residues, form the S3 pocket of RgpB. The replacement of Tyr390 existing in Kgp with Gly154 in RgpB and the close spatial location of Ser156 in RgpB (Figure 2D) make the S3 pocket of the latter more shallow and larger.

Structure-Based Design of Gingipain Inhibitors. The availability of the X-ray structure of RgpB (the complex with FFR−CH_2Cl, encoded as 1CVR in PDB) and the 3D model of Kgp allowed us to use structure-based design methods for the development of new gingipain inhibitors. For this purpose the computer program LUDI[34,35,39,40] was employed to find new substituents from the LUDI_Link library (about 1500 molecular fragments) at the P2 and/or P3 positions of gingipain ligands. According to the analysis presented in the preceding section, the P1 residues were strictly conserved: Arg for RgpB and Lys for Kgp. The chloromethyl ketone moiety, reactive versus the catalytic cysteine thiolate, was selected intentionally to ensure binding of the inhibitors to the enzyme active site.

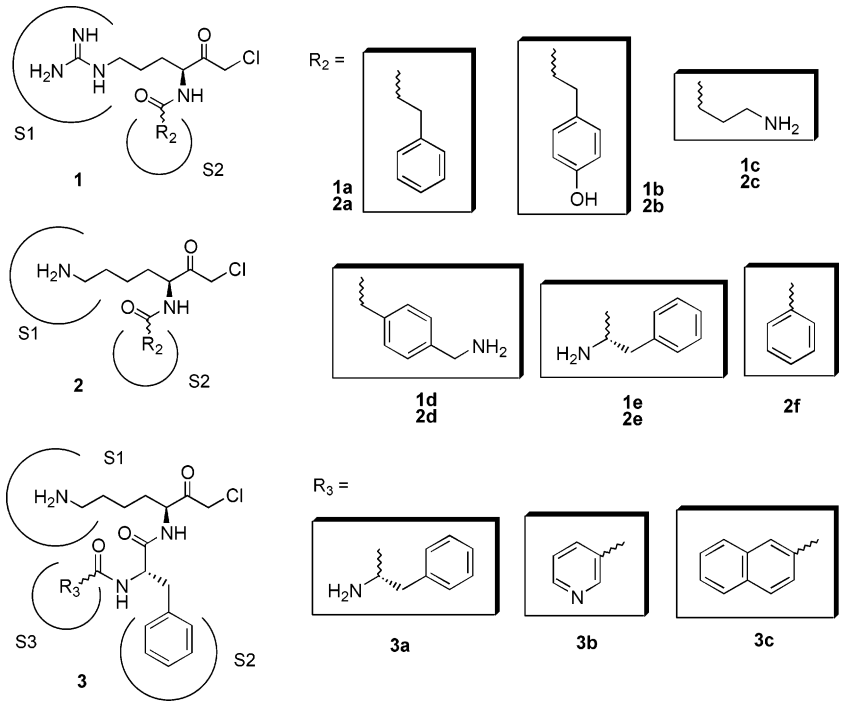

Figure 3. Structures of the designed P2 and P3 substituents of chloromethyl ketone inhibitors of gingipains containing the arginine or lysine residue at P1 (**1**−**3**).

The structures of novel RgpB ligands were designed in such a way that the P2 side chain of FFR-CH_2Cl was replaced with substituents found by LUDI, whereas the P3 residue was removed. A systematic search of the LUDI_Link library, docking, and analysis of the potential interactions with the S2 pocket allowed us to identify the substituents interacting favorably with this region. Various molecular fragments of hydrophobic and/or basic character inserted between Tyr283 and Asp281 were found in this way. They can be involved in hydrophobic contacts with both amino acids and form a hydrogen bond with carboxylate of the Asp281 side chain. A series of chloromethyl ketone dipeptides designed in this manner were selected for synthesis and subsequently tested for their affinity toward RgpB (**1a**−**e**, Figure 3 and Table 1). We did not proceed with their further elongation due to the character and spatial arrangement of the S3 pocket of RgpB: shallow and widely open to solvent.

To design Kgp inhibitors, initially we docked L-Phe-Phe-Lys-CH_2Cl (FFK-CH_2Cl) to the homology built model, utilizing this complex for further modifications. As a result, two series of inhibitors containing different substituents at the P2 and P3 positions found in the LUDI_Link library were developed (**2a**−**f**, **3a**−**c**, Figure 3). Interestingly, the residues identified as favorable at P2 of Kgp dipeptide ligands appeared to be virtually the same as the corresponding substituents designed for RgpB. This results from a high similarity of the S2 pockets in both gingipains. Since we kept the oxygen atom of Asn510 in Kgp oriented toward P2 of the ligand, this region in both enzymes remained indistinguishable for the interacting ligands. Surprisingly, the structure−activity relationship for RgpB and Kgp inhibitors bearing the same substituents at P2 (**1a**−**e** and **2a**−**e**) differs significantly (see below for details).

Because the S3 pocket in Kgp seems to be relatively deeper than the corresponding one in RgpB, we proceeded with the design of tripeptide analogues as potential Kgp inhibitors. In the RgpB−FFR-CH_2Cl complex, the S3 pocket remains empty because Phe at the *N*-terminus of the ligand possesses the D configuration and is entirely solvent exposed. In the case of Kgp, the L-FFK-CH_2Cl diastereoisomer was docked into the binding site and subsequently its *N*-terminal residue was replaced with new substituents from the LUDI_Link library to occupy the S3 pocket. Most of the designed P3 ligands were bulky aromatic residues, which could nestle close to the Trp513 and Tyr390 side chains. Three of the tripeptide analogues were selected for synthesis and in vitro tests toward Kgp (**3a**−**c**, Figure 3).

Table 1. Inhibition of Gingipains by Chloromethyl Ketone Derivatives (**1**−**3**)[a]

	Gingipain R R_2CO-Arg-CH_2Cl		R_2		Gingipain K R_2CO-Lys-CH_2Cl	
	k_{obs} (s^{-1})	$k_{obs}/[I]$ ($M^{-1}s^{-1}$)			k_{obs} (s^{-1})	$k_{obs}/[I]$ ($M^{-1}s^{-1}$)
1a	0.00298 ± 0.00021	1260000 ± 152000		**2a**	0.0431 ± 0.0045	4460000 ± 690000
1b	0.05878 ± 0.003	25100000 ± 2540000	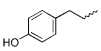	**2b**	0.0554 ± 0.002	848000 ± 73200
1c	0.07858 ± 0.0109	33200000 ± 6270000		**2c***	0.0572 ± 0.0112	1060 ± 262
1d	0.04055 ± 0.0061	16900000 ± 3390000	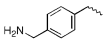	**2d***	0.000954 ± 0.00021	132 ± 35.7
1e	0.00283 ± 0.00029	1240000 ± 189000		**2e***	0.00481 ± 0.001	115 ± 29.8
				**2f**	0.1020 ± 0.0115	11500000 ± 1880000
			R_3		R_3CO-Phe-Lys-CH_2Cl	
				**3a***	0.0108 ± 0.0023	279 ± 73.2
				**3b**	0.0112 ± 0.0013	105000 ± 17600
				**3c**	0.0151 ± 0.0017	267000 ± 43400

[a] The asterisk (∗) indicates that the deviation from the linear dependence of $-\ln(v/v_0)$ versus time was observed.

Scheme 1[a]

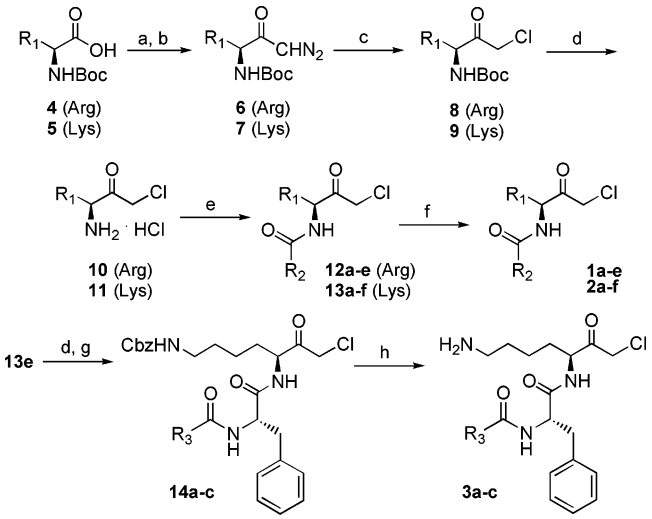

[a] Reagents and conditions: (a) *i*-BuOCOCl, NMM, anhydrous THF, −18 °C; (b) CH_2N_2; (c) 2.5 M HCl/MeOH; (d) 7.5 M HCl/MeOH; (e) R_2COCl, NMM, anhydrous THF, 0 °C, or R_2COOH, *i*-BuOCOCl, NMM, anhydrous THF, 0 °C; (f) TFA/thioanisol (9:1, arginine derivatives) or TFA/anisol (9:1, lysine derivatives) and then HPLC; (g) R_3COOH, *i*-BuOCOCl, NMM, anhydrous THF, 0 °C, or R_3COCl, NMM, anhydrous THF, 0 °C; (h) TFA/anisol (9:1) and then HPLC (for structures of R_2 and R_3 substituents, see Figure 3).

Chemistry. The synthesis of the designed compounds started from the suitably protected derivatives of lysine and arginine (**4**, **5**) (Scheme 1). Their carboxylate function were converted consequently into the diazomethyl (**6**, **7**) and chloromethyl ketone derivatives (**8**, **9**) in a standard way. Then the α-amino group, after selective deprotection, was acylated by appropriate mixed anhydrides or chloridates, giving dipeptide analogues (**12a**−**e**, **13a**−**f**). The latter step could be done in parallel for different derivatives. This was the reason we selected such an option[41] rather than the synthesis of the whole sequences followed finally by their transformation into chloromethyl ketones. For tripeptides (**14a**−**c**) the derivatization occurred on the Phe-Lys-CH_2Cl conservative structure. All the final protected compounds (**12**−**14**) were purified by column chromatography, separated as crystalline compounds, and characterized (for details, see the Supporting Information).

The mildest conditions for the benzyloxycarbonyl group removal were catalytic hydrogenation. However, in case of chloromethyl ketones it leads to their reduction and conversion into methyl ketones. Thus, various acidic hydrolysis conditions were tested. For lysine derivatives (**13**, **14**), 10% anisol/TFA for 24 h at room temperature gave satisfactory results. Arginine compounds (**12**) appeared much more resistant, which was additionally dependent on their structure. Finally, 10% thioanisol/TFA was the reagent of choice. The target inhibitors (**1**−**3**) were obtained after their purification on reverse phase HPLC. Their purity (exceeding 95%) was verified by analytical HPLC experiments.

Interactions of Inhibitors with RgpB: Structure−Activity Relationship. Inactivation of gingipains by the designed compounds was investigated under pseudo-first-order conditions (Figure 4) in which proteinases were mixed with a large excess of inhibitors.

In general, all the tested arginine chloromethyl ketones (**1a**−**e**) appeared to be very potent irreversible inhibitors of RgpB, with $k_{obs}/[I]$ values in the range of 10^6-10^7 M^{-1} s^{-1} (Table 1), showing unambiguously that dipeptide analogues are sufficiently extended to achieve high affinity. Four out of five compounds

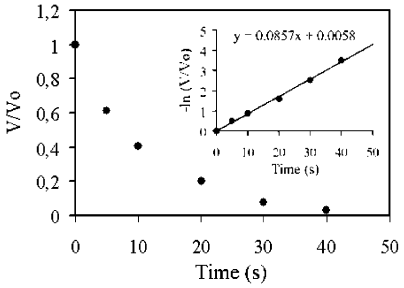

Figure 4. Time dependence of RgpB inhibition by **1c** under pseudo-first-order conditions. The insert shows k_{ass} calculation from the plot of $-\ln(v/v_0)$ against time.

(**1a**−**d**) lack the *N*-terminal α-amino group. In accordance to the interaction mode of FFR-CH_2Cl with RgpB, this group is not involved in any interaction with the protein. Indeed, the binding affinity of **1e** ($k_{obs}/[I] = 1.24 \times 10^6$ M^{-1} s^{-1}), the only RgpB ligand bearing the *N*-terminal α-amino group, is the same as that observed for **1a**, which has the identical structure but is missing this group ($k_{obs}/[I] = 1.26 \times 10^6$ M^{-1} s^{-1}). More significantly, designed ligands bearing a polar group at P2 (**1b**−**d**) appeared to be 10−30-fold more potent than the analogue with a phenylethyl group at P2 (**1a**), although the latter one, together with other hydrophobic residues (Val, Pro), was considered an optimal substituent at the P2 position.[20,26,28] Compound **1c**, bearing a short, positively charged 3-aminopropyl at P2, exhibited the most potent inhibition of RgpB ($k_{obs}/[I] = 3.32 \times 10^7$ M^{-1} s^{-1}, Figure 4). This represents a 25-fold increase in potency compared to **1a** (Table 1). According to the interaction model, the side chain amino group of **1c** can form favorable electrostatic interactions with the carboxyl group of Asp281 (Figure 5A). Furthermore, hydrophobic interactions with the S2 residues make the 3-aminopropyl group the most effective P2 substituent of RgpB ligands. The incorporation of (*p*-hydroxyphenyl)ethyl at the corresponding position (**1b**) also leads to a high inhibition rate ($k_{obs}/[I] = 2.51 \times 10^7$ M^{-1} s^{-1}), comparable to that of **1c** when taking into account the uncertainties (Table 1). The P2 hydroxy group can be involved in the hydrogen bond with Asp281, increasing the affinity of **1b** by 20-fold if compared to **1a**, which is missing one. The interaction pattern of **1d**, containing a (*p*-aminomethyl)benzyl group ($k_{obs}/[I] = 1.69 \times 10^7$ M^{-1} s^{-1}), is expected to be similar to those of **1b** and **1c**. In summary, the most favorable substituents at P2 are simultaneously comprised of a hydrophobic part and a polar group, particularly positively charged, which is able to serve as a hydrogen-bond donor. Lack of interactions with the carboxyl group of Asp281 results in decreased affinity by more than 1 order of a magnitude.

The necessity of appropriate size and basicity of P2 substituents of RgpB ligands is consistent with the presence of Lys and Arg in RgpB substrates, such as human histatins for their effective cleavage by RgpB.[8] Furthermore, the potent RgpB inhibitor **16**, which is a tetrapeptide analogue, also contains Lys at the P2 position.[8] However, the molecular roots of its high potency have not been revealed thus far. Here, we propose the structural basis for the interactions of amino acids forming the S2 pocket of RgpB with the corresponding fragment of the interacting ligand, both substrates and inhibitors.

Interactions of Inhibitors with Kgp: Structure−Activity Relationship. Most of the dipeptide analogues tested toward Kgp exhibit lower potency than the corresponding arginine derivatives toward RgpB (Table 1). Interestingly, inhibitors **2a**, **2b**, and **2f** are potent, with $k_{obs}/[I]$ values up to 10^7 M^{-1} s^{-1}, while the remaining three, **2c**, **2d**, and **2e**, show much weaker

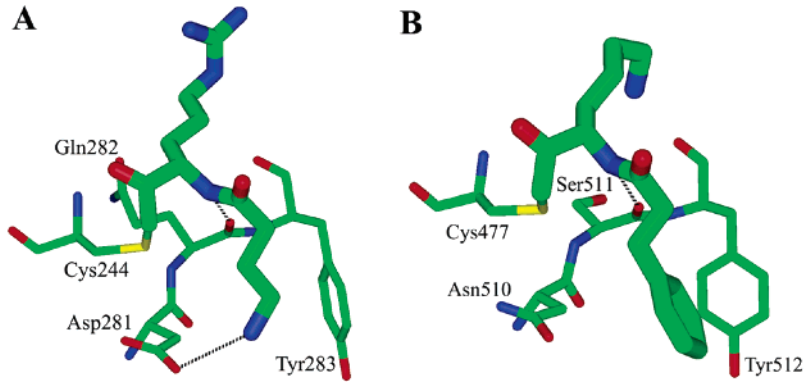

Figure 5. Modeled interaction mode of **1c** with RgpB (panel A) and **2a** with Kgp (panel B), with particular attention to the interactions of P2 substituents with the S2 binding pockets of gingipains.

affinity. Furthermore, the Kgp inhibitors reveal different patterns in their structure−activity relationship if compared to RgpB ligands bearing the same substituent at P2. This can be attributed to a single difference in the S2 pocket: Asp281 in RgpB is replaced by neutral Asn510 in Kgp, changing the character of the S2 pocket. The detailed analysis of the intramolecular interactions in Kgp revealed that the oxygen atom of the Asn510 side chain is most likely involved in the hydrogen bond with the backbone amide of the same residue. This would keep the NH_2 group of Asn510 directed toward the P2 side chains of the interacting ligands, modifying binding preferences of the S2 pocket of Kgp versus RgpB.

The analogues with the hydrophobic groups at P2 revealed the highest inhibition rate among all compounds tested toward Kgp. Incorporation of the benzoyl at P2 (**2f**, $k_{obs}/[I] = 1.15 \times 10^7$ M^{-1} s^{-1}) increases the affinity by 220-fold if compared to the chloromethyl ketone analogue of lysine (not presented in Table 1, Lys-CH_2Cl, $k_{obs}/[I] = 5.25 \times 10^4$ M^{-1} s^{-1}). Since the P2 carbonyl group is not involved in any hydrogen bond with Kgp (Figure 2B), it does not contribute to the binding affinity. Therefore, the difference between Lys-CH_2Cl and **2f** results only from the favorable interactions of the phenyl group with the hydrophobic part of the Asn510 side chain and with the backbone of 510−512 residues. Although extension of the P2 side chain to the phenylethyl group (**2a**) is expected to be reflected in more hydrophobic contacts with Kgp (Figure 5B) in comparison to **2f**, increased potency is not observed ($k_{obs}/[I] = 4.46 \times 10^6$ M^{-1} s^{-1}), which might result from the increased flexibility of **2a**. The incorporation of (*p*-hydroxyphenyl)ethyl at P2 (**2b**) enhances the affinity 16 times versus Lys-CH_2Cl; however, **2b** still binds about 5-fold weaker to Kgp than **2a**. This result suggests that the hydroxy group of **2b** is not engaged in any hydrogen bond with the S2 pocket. Additionally, this finding supports an idea that the NH_2 group rather than the oxygen atom of the Asn510 side chain amide is oriented toward P2 of the ligand (the reverse orientation was originally selected for the ligand design procedure). Due to undesirable geometry, the hydroxy group at P2 of **2b** cannot also serve as the hydrogen-bond acceptor for NH_2 of Asn510. Our finding that the hydrogen-bond-donor group is unfavorable at P2 of potential ligands is consistent with the substrate specificity of Kgp. The enzyme efficiently cleaves human histatins with Glu at P2 compared to Tyr or Ala at the corresponding position.[8]

Compounds with a positively charged amino group at P2 (**2c** and **2d**), as well as the analogues with free *N*-terminal amino group (**2e** and **3a**), are at least 50 times less potent than Lys-CH_2Cl toward Kgp. Although weak affinity of **2c** and **2d** might be explained in the same way as for **2b**, the difference of four orders of a magnitude between **2e** and **2a** is surprising (corresponding arginine derivatives: **1e** and **1a** do not differ in the affinity toward RgpB, Table 1). Interestingly, the observed inactivation of Kgp measured in the presence of **2c**−**e** and **3a** was unlike the remaining analogues, namely a deviation from linear dependence of $-\ln(v/v_0)$ versus time was observed. This might suggest nonspecific binding of these compounds to Kgp, to the region displaced from the substrate binding site. Their common feature is the presence of an additional positively charged amino group, either at P2 (**2c** and **2d**) or at the *N*-terminus of di- or tripeptide analogues (**2e** and **3a**), besides Lys at P1. On the basis of the predicted binding mode of the inhibitors to the binding site of Kgp, no structural explanation can be found to clarify why the existence of the *N*-terminal amino group in **2e** and **3a** decreases the affinity by as much as 40 000 times (compare **2e** and **2a**). Both in dipeptide and tripeptide analogues, it is expected to be solvent exposed and not involved in any interactions with the enzyme, in the same manner as the backbone amide of P2 and the *N*-terminal amino group of P3 in FFR-CH_2Cl interacting with RgpB.[38] Nonspecific binding of **2c**−**e** and **3a** to Kgp through positively charged moieties might represent an explanation for this observation.

As the S3 pocket in Kgp was presumed to be deeper than in RgpB (Figure 2D), the tripeptide analogues bearing different substituents at P3 were designed to explore this pocket. Three of them (**3a**−**c**) were selected for synthesis and tested toward Kgp. In general, the incorporation of an additional P3 residue decreases the affinity of the tested compounds if compared to the dipeptide derivatives. The analogues **3b** and **3c** are respectively 40 and 17 times weaker than **2a**, which they originate from (Table 1). Although the 2-naphthyl substituent at P3 (**3c**) is expected to form the hydrophobic interactions with Trp513 and Tyr390, it would be solvent exposed from another side. The pyridine substituent of **3b** is considered to interact with Trp513 and to form a hydrogen bond with the side chain hydroxy group of Tyr390. It is difficult to conclude whether the predicted interactions actually take place. The potential energetic gain might be used to compensate the unfavorable entropy effects originating from the presence of the flexible portion, namely, the backbone of P2 and P3 residues, which is not expected to form hydrogen bonds with Kgp.

Structure−Activity Relationship for Known Gingipain Inhibitors. The above-presented analysis of interactions between Kgp and its synthetic inhibitors (**2a**−**f** and **3a**−**c**) supports the reliability of the constructed 3D model of gingipain K. To further validate these results, the structure−activity relationship for other known Kgp inhibitors (Figure 6) was analyzed. One of the most potent compounds identified so far, ketopeptide **17** ($K_i = 7.5 \times 10^{-11}$ M),[8] was selected for detailed analysis of its interactions with Kgp. According to our model of the Kgp−**17** complex, it

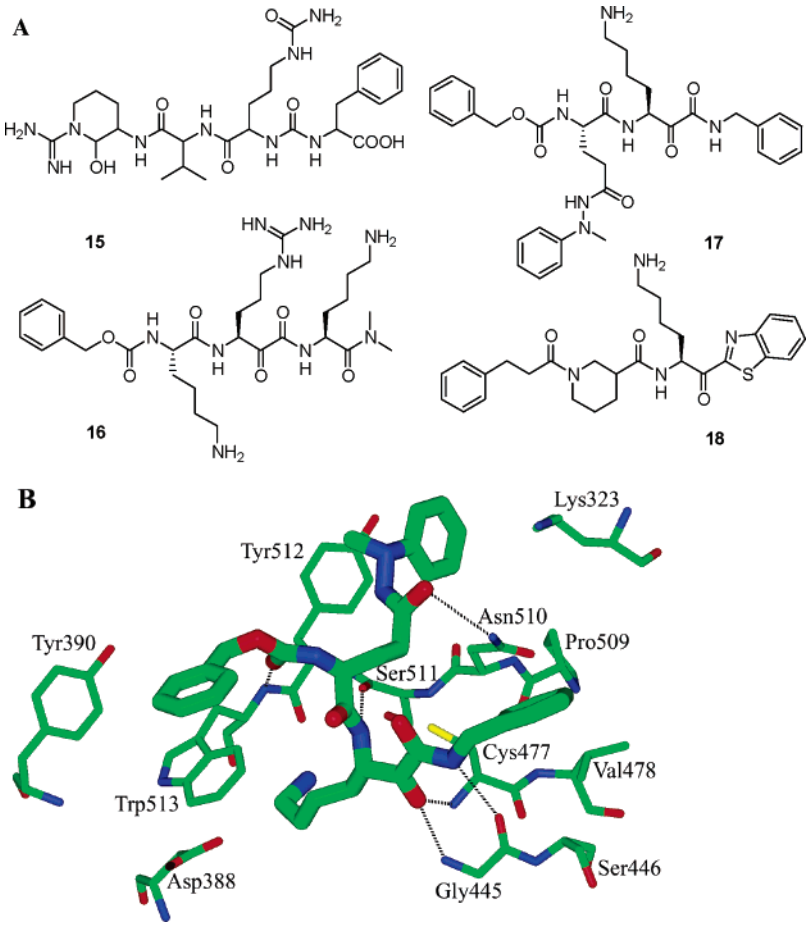

Figure 6. Structures of known, natural, and synthetic inhibitors of gingipain R (**15** and **16**) and gingipain K (**17** and **18**) (A).[8,26,29] Modeled binding mode of **17** (thicker bonds colored according to atom types) to Kgp; residues of the S1 pocket are not shown for clarity of the figure (B).

is engaged in a remarkable interaction pattern with the enzyme (Figure 6B). All backbone−backbone hydrogen bonds observed for inhibitors **2** and **3** are retained, and additional ones with Gly445 and Trp513 are formed. The Lys amino group at P1 is expected to be involved in a similar hydrogen bond network as described above (Figure 2B). The P2 side chain fits very well in the S2 pocket, as a hydrogen bond with the Asn510 amide, and hydrophobic interactions with the Tyr512, Asn510, Lys323, and Pro509 side chains are present. The P3 side chain of **17** is accommodated very well in the S3 hydrophobic pocket, interacting with Trp513, Tyr390, and Asp388. In addition, the P1′ fragment of **17** (absent in inhibitors described in this paper) is positioned in a favorable orientation for a hydrogen bond with Gly445 and for hydrophobic interactions with Val478, Cys477, and Asn510.

The Kgp model can also be applied to explain SAR for other Kgp inhibitors described in the literature, including compound **18**[29] (Figure 6A). In addition to the backbone−backbone hydrogen bond network and interactions engaging Lys at P1, the remaining fragments of **18** seem to fit well to the corresponding pockets of Kgp. The S2 Asn510 should be able to form hydrophobic contacts with the heterocyclic part of the ligand, whereas both the P3 and P*n*′ portions are expected to interact with Kgp in a similar way as the corresponding fragments of **17**. Other reported Kgp inhibitors, aza-peptide Michael acceptors ($PhCH_2CH_2CO$-Leu-ALys-CH=CHCOOEt)[30] and peptidyl chloromethyl and acyloxymethyl ketones (Cbz-Phe-Lys-CH_2Cl and Cbz-Phe-Lys-CH_2OCO-2,4,6-Me_3Ph),[28] contain hydrophobic P2 and P3 substituents. All these findings are consistent with the proposed binding mode of Kgp ligands, supporting our 3D model of Kgp.

The molecular basis of binding affinity of synthetic inhibitors **1a**−**e** toward RgpB is entirely relevant for other known inhibitors of this enzyme. Compounds reported in the literature exhibiting reasonably strong potency contained either a hydrophobic substituent (**15**,[26] D-Phe-Pro-Arg-CH_2Cl, D-Phe-Phe-Arg-CH_2Cl[28]) or a Lys side chain (**16**)[8] at P2 (Figure 6A). This remains in good agreement with our findings concerning the binding preferences of gingipain R discussed here.

Conclusions

In summary, our study represents the first example of the rational development of gingipain inhibitors by applying the structure-based design approach using the X-ray structure of RgpB and the 3D model of Kgp. High affinity of obtained compounds toward both enzymes ($k_{obs}/[I] \sim 10^7\ M^{-1}\ s^{-1}$) was achieved for the dipeptide analogues, without the necessity of a further increase of the ligand size. Currently, all potent inhibitors of RgpB and Kgp reported in the literature represent more extended structures.[20] Moreover, we found that Kgp and RgpB inhibitors bearing the same substituent at P2 show a different pattern in their structure−activity relationship. Molecular fragments containing a hydrogen-bond-donor group, particularly the amino group at P2, are the best ligands for RgpB, whereas Kgp prefers hydrophobic ones.

The comparative analysis of the binding pockets in Kgp and RgpB revealed the structural basis of differences in ligand−enzyme interactions. The substrate specificity of gingipains originates mostly from the different size and character of their

S1 pockets, dedicated to exclusively accommodate the Lys or Arg residues. In addition, distinct preferences of the S2 pockets were recognized in both gingipains. They result from the replacement of negatively charged Asp281 in RgpB with neutral Asn510 in Kgp. These molecular roots of substrate recognition explain the specificity of gingipains toward their natural substrates, including human histatines, in which different cleavage sites have been found for RgpB and Kgp.[8]

The binding affinity data we report as well as those found in the literature for Kgp ligands confirm the good quality of our 3D model of the enzyme and its usefulness for structure based drug design. Although the sequence identity of Kgp to the template protein (RgpB) is modest (below 30%), our model makes it possible to explain the structure−activity relationship for Kgp ligands. A similar approach was successfully applied in our previous studies on aminopeptidase N and phenylalanine ammonia lyase inhibitors.[42,43]

It has to be emphasized that, due to their high reactivity, chloromethyl ketones are not suitable for in vivo studies. Here, these model compounds have been explored to get insight into the S*n* binding pockets and to recognize the structural preferences of both gingipains in these regions. The knowledge arising from the presented studies will subsequently serve to develop new classes of less reactive and more selective RgpB and Kgp inhibitors, including compounds much more complex for synthesis, such as epoxides. Their structures offer an attractive opportunity for the extension at the P*n*′ portion to interact with the S*n*′ regions of both proteases. This will open an avenue toward the development of therapeutically useful inhibitors targeting gingipains for the treatment of periodontal diseases.

Experimental Section

Homology Modeling of Kgp. The amino acid sequence of Kgp is available from the National Center for Biotechnology Information (NCBI, www.ncbi.nlm.nih.gov, gi number 1314751). The search for homologous proteins in Protein Data Bank was performed using the BLAST program (www.ncbi.nlm.nih.gov/blast). This resulted in one protein, RgpB (encoded as 1CVR in PDB), with reasonable sequence similarity to Kgp (26% sequence identity and 40% sequence similarity for the for 231−680 amino acid fragment, which includes the catalytic domains of Kgp). The pairwise sequence alignment of Kgp and RgpB was performed using ClustalW (http://www.ebi.ac.uk/clustalw) with a few manual corrections. This alignment was then applied to calculate the 3D model of the catalytic domain of Kgp (residues 231−680) by employing the Modeller program[37] (http://salilab.org/modeller.html) with the default parameters.

Design and Docking of New Inhibitors of RgpB and Kgp. The X-ray structure of RgpB in complex with D-Phe-Phe-Arg-CH_2-Cl (FFR-CH_2Cl; structure encoded as 1CVR in PDB) was used to design new inhibitors of RgpB by employing the computer program LUDI/Insight II (Accelrys).[40] The hydrogen atoms were added to RgpB and FFR-CH_2Cl in the program InsightII/Builder[44] using the standard protonation states for amino acids at pH 7.0. New inhibitors were designed by replacing the Phe side chain at P2 of FFR-CH_2-Cl with new substituents from the LUDI_Link library (about 1500 structural fragments) and removing the P3 residue. New fragments, which fit sterically and electrostatically to the enzyme binding pocket, were selected as 'hits'. The values of the most important LUDI parameters used for the design of new RgpB inhibitors were as follows: Min Separation = 3; Link, Lipo, and H−Bond Weights were set to 1.0; Aliphatic_Aromatic and Reject Bifurcated parameters were turned off; No_Unpaired_Polar, Electrostatic_Check, and Invert parameters were turned on; Es Dist = 2.5; Max RMS = 0.5; Number of Rotatable Bonds, two at a time; and Radius of Search was changed from 5 to 10 Å. Visual inspection of the interactions between the designed inhibitors and RgpB was performed within the program Insight_1997. Subsequently, the protein was soaked in a 5-Å layer of water molecules and the complex of RgpB with each designed inhibitor was optimized in the cff91 force field using Discover/InsightII.[45] The backbone of the protein was kept frozen during the optimization process, while the protein side chains, inhibitor molecules, and water were allowed to move. The distance constrains with the force constant values 500 kcal/mol Å^2 were applied during the minimization to keep the backbone−backbone hydrogen-bond network existing in the RgpB−FFR-CH_2Cl complex.[38] The switched smoothing function, with gradually reduced nonbonding interactions to zero from 18 Å inner and 20 Å outer radius, was applied during the simulations. The energy minimization procedure was performed using the conjugate gradient algorithm until the maximum derivative was below 0.1 kcal/mol.

The hydrogen atoms were added to Kgp model in InsightII/Builder, using the standard protonation states for amino acids at pH 7.0. The model of RgpB−FFR-CH_2Cl complex served to dock L-Phe-Phe-Lys-CH_2Cl (FFK-CH_2Cl) to the Kgp binding site by superimposition of the RgpB−FFR-CH_2Cl onto the Kgp model. The Arg side chains of FFR-CH_2Cl was then replaced with a Lys side chain and the complex Kgp−FFK-CH_2Cl was optimized using the same procedure as described for RgpB inhibitors. New chloromethyl ketone inhibitors of Kgp with different substituents at P2 and P3 positions were designed in the same way as described for RgpB inhibitors. The model of Kgp with compound **17** was built on the basis of the position of FFK-CH_2Cl in the Kgp binding site. The backbone and P1 Lys were retained as in FFK-CH_2Cl, the P2 and P3 side chains were rebuilt manually using the appropriate fragments from InsightII/Builder fragment library, and the P*n*′ part of **17** (absent in FFK-CH_2Cl) was added from the same library. The Kgp−**17** complex was then soaked in water and optimized in the same way as described for RgpB inhibitors.

Chemistry−General. Unless otherwise stated, materials were obtained from commercial suppliers (Sigma-Aldrich, Novabiochem, Fluka, Merck, POCh) and used without purification. Isobutyl chloroformate and thionyl chloride were freshly distilled. Anhydrous THF was obtained by its heating over Na/benzophenon and distilled before using. Column chromatography was performed on silica gel 60 (70−230 mesh).

Melting points were determined on Boetius apparatus and were not corrected. IR spectra were recorded for KBr pellets or on film on a Perkin-Elmer System 2000 FT IR spectrometer. Proton spectra were recorded on Bruker DRX spectrometer operating at 300.13 MHz. Measurements were made in $CDCl_3$ or D_2O solutions. Proton chemical shifts are reported in relation to tetramethylsilane used as internal standard. Preparative HPLC separation and analytical purity verification were performed on Varian ProStar apparatus with ProStar 325 UV/Vis detector using Dynamax 250 × 21.4 Microsorb 300-10 C18 and 250 × 4.6 Microsorb-MV 100-5 C18 columns, respectively. A and B mobile phases refer to water and acetonitrile, respectively, both containing 0.1% TFA. Elemental analyses were performed at the Laboratory of Instrumental Analysis, University of Wrocław on Elementar vario EL III apparatus.

General Procedure for Preparation of Boc-Arg(Z)$_2$-CH_2Cl and Boc-Lys(Z)-CH_2Cl (8, 9).[46] A mixed anhydride was prepared by addition of isobutyl chloroformate (3.9 mL, 30 mmol) to a solution of Boc-Arg(Z)$_2$−OH (**4**) or Boc-Lys(Z)-OH (**5**) (25 mmol) and *N*-methylmorpholine (NMM, 3.44 mL, 31.25 mmol) in anhydrous THF (150 mL) at −18 °C. After 1 h of stirring the precipitated ammonium salt was filtered off under nitrogen atmosphere. Then diazomethane prepared from *p*-toluenesulfonyl-*N*-methyl-*N*-nitrosoamide (10.7 g, 50 mmol) was distilled with ether (∼100 mL) directly to the filtrate cooled to 0 °C. The resulting mixture was kept at −18 °C overnight. Solvents were removed under reduced pressure, the oily residue of a diazomethyl ketone (**6**, **7**) was redissolved in 100 mL of THF and treated with 2.5 M methanol solution of HCl (10 mL, 25 mmol). The reaction progress was controlled by TLC analysis (ethyl acetate/hexane, 2:3). Subsequent removal of solvents gave a crude product as dense oil.

Crystallization from an ethyl acetate/hexane yielded a pure chloromethyl ketone as a crystalline white solid.

General Procedures for Preparation of the Protected Chloromethyl Ketones: R_2-Arg(Z)$_2$-CH_2Cl (12), R_2-Lys(Z)-CH_2Cl (13), and R_3-Phe-Lys(Z)-CH_2Cl (14). Method A: Acylation with an Appropriate Acid Chloride. H-Arg(Z)$_2$-CH_2Cl (**10**), H-Lys(Z)-CH_2Cl (**11**), or H-Phe-Lys(Z)-CH_2Cl hydrochloridates were obtained from Boc-Arg(Z)$_2$-CH_2Cl (**8**), Boc-Lys(Z)-CH_2Cl (**9**), or Boc-Phe-Lys(Z)-CH_2Cl (**13e**) (2 mmol), respectively, dissolved in a minimum quantity of THF and treated with an excess of 7.5 M HCl in methanol (13.4 mL, 10 mmol) within 40 min for arginine and 15 min for lysine derivative at 0 °C. After evaporation, the obtained salt was suspended in anhydrous THF (30 mL). *N*-Methylmorpholine (0.55 mL, 5 mmol) and an acid chloridate (2.4 mmol, 5 min later) were added consecutively to the stirred mixture and cooled in a water/ice bath. Acid chloridates were either commercial or synthesized from the appropriate acid upon reaction with thionyl chloride in the standard way. After 24 h of stirring, the mixture was concentrated under reduced pressure. The residue was taken up with ethyl acetate (50 mL) and water (10 mL) and washed consecutively with 5% $NaHCO_3$ (40 mL), 5% citric acid (2 × 40 mL), and brine (40 mL). The organic layer was then dried over anhydrous Na_2SO_4. After removal of the solvent, the residue was purified on silica gel column. A solution of ethyl acetate/hexane was used as the eluent. The obtained material was additionally recrystallized from an ethyl acetate/hexane mixture, giving pure chloromethyl ketones as white crystals.

Method B: Mixed Anhydrides. To a stirred solution of an acid (2 mmol) in anhydrous THF (50 mL) were added NMM (0.55 mL, 5 mmol) and isobutyl chloroformate (0.31 mL, 2.4 mmol) at 0 °C. Stirring was continued for 45 min. Then H-Arg(Z)$_2$-CH_2Cl (**10**), H-Lys(Z)-CH_2Cl (**11**), or H-Phe-Lys(Z)-CH_2Cl hydrochloridate (2 mmol, obtained as described above for method A) suspended in anhydrous THF (30 mL) was added. After 24 h of stirring, the mixture was worked up and purified the same manner as described above.

Deprotection. Removal of the N^{ϵ}-benzyloxycarbonyl residue from the lysine derivatives was achieved under acidic conditions of 10% anisol in trifluoracetic acid mixture at ambient temperature for 24 h. For deprotection of arginine N^{δ}- and N^{ω}-benzyloxycarbonyl residues, thioanisol was applied in place of anisol. A 2-mL portion of solution was used for 0.1 mmol of a chloromethyl ketone. After completion of the reaction, TFA was evaporated, and the residue was worked up with water (HPLC grade) and washed three times with ether. The water phase was concentrated and the resulting mixture was applied on preparative HPLC. The collected samples were lyophilized. Their purity and homogeneity were verified by analytical HPLC.

Determination of the Residual Activity of Gingipains—General. Substrates Tos-Gly-Pro-Arg-AMC and Tos-Gly-Pro-Lys-AMC were purchased from Bachem (Switzerland); all other reagents were purchased from Sigma. Substrates were dissolved in DMSO. Inhibitors were dissolved in MiliQ water or DMSO. Final stock solutions were diluted in the reaction buffer.

Activation of Gingipains. RgpB and Kgp were purified from *P. gingivalis* HG66 culture medium as described by Pike et al.[11] The enzymes were activated with 10 mM cysteine in 50 mM HEPES (pH 7.5), 10 mM $CaCl_2$ for 15 min at 37 °C. The activated proteases were diluted with reaction buffer [0.1 M Tris (pH 7.5), 0.15 M NaCl, 10 mM $CaCl_2$, 10 mM cysteine, 0.025% Triton X-100] prior to use.

Inhibition Assays. The rate of gingipain inactivation was measured under pseudo-first-order conditions: the concentration of an inhibitor exceeded the protease concentration by at least 10 times. A 50-μL aliquot of the activated enzyme was mixed with 5−15 μL of an inhibitor solution, incubated at 21 °C for the 5−180 s, and diluted at least 15 times with the reaction buffer containing substrate. The final concentration of Tos-Gly-Pro-Arg-AMC and Tos-Gly-Pro-Lys-AMC substrates was 1.5×10^{-6} and 7.0×10^{-6} M, respectively. Residual enzyme activity was measured with an FP-750 spectrofluorimeter (Jasco) for 150 s. Excitation at 355 nm and emission at 445 nm were used to maximize the free AMC (7-amino-4-methylcoumarin) fluorescence signal. First-order inactivation rate constants (k_{obs}) were obtained from the plots showing the dependence of $-\ln(v/v_0)$ versus time. The second-order rate constant (k_{ass}) was calculated from the equation $k_{ass} = k_{obs}/[I]$. The measurements were repeated at least twice for every compound tested. Mean values of k_{ass}, which differed by less than 20% for potent inhibitors ($k_{obs}/[I] > 10^4$ M^{-1} s^{-1}) and less than 30% for weaker ligands, were calculated for every compound.

Acknowledgment. This work is supported by the Committee of Scientific Research (KBN, Poland, grant 6 P04B 025 21). J.P. acknowledges grants DE 09761 and 3 P04A 003 24 from the National Institutes of Health and the Committee of Scientific Research (KBN, Poland), respectively. J.P. was the recipient of an award SUBSYDIUM PROFESORSKIE from the Foundation for Polish Science (FNP, Warszawa, Poland). We thank Rachael Riley and David Shultis (University of Virginia, Charlottesville) for critical reading of the manuscript.

Supporting Information Available: NMR, IR, and elemental analysis data and HPLC chromatograms of the protected and final products. This material is available free of charge via the Internet at http://pubs.acs.org.

References

(1) DeStefano, F.; Anda, R. F.; Kahn, H. S.; Williamson, D. F.; Russell, C. M. Dental disease and risk of coronary heart disease and mortality. *Br. Med. J.* **1993**, *306*, 688−691.
(2) Beck, J. D.; Pankow, J.; Tyroler, H. A.; Offenbacher, S. Dental infections and atherosclerosis. *Am. Heart J.* **1999**, *138*, S528−533.
(3) Scannapieco, F. A. Role of oral bacteria in respiratory infection. *J. Periodontol.* **1999**, *70*, 793−802.
(4) Teng, Y. T.; Taylor, G. W.; Scannapieco, F.; Kinane, D. F.; Curtis, M.; et al. Periodontal health and systemic disorders. *J. Can. Dent. Assoc.* **2002**, *68*, 188−192.
(5) Shapira, L.; Ayalon, S.; Brenner, T. Effects of *Porphyromonas gingivalis* on the central nervous system: Activation of glial cells and exacerbation of experimental autoimmune encephalomyelitis. *J. Periodontol.* **2002**, *73*, 511−516.
(6) Romero, B. C.; Chiquito, C. S.; Elejalde, L. E.; Bernardoni, C. B. Relationship between periodontal disease in pregnant women and the nutritional condition of their newborns. *J. Periodontol.* **2002**, *73*, 1177−1183.
(7) Jeffcoat, M. K.; Hauth, J. C.; Geurs, N. C.; Reddy, M. S.; Cliver, S. P.; et al. Periodontal disease and preterm birth: Results of a pilot intervention study. *J. Periodontol.* **2003**, *74*, 1214−1218.
(8) Kadowaki, T.; Baba, A.; Abe, N.; Takii, R.; Hashimoto, M.; et al. Suppression of pathogenicity of *Porphyromonas gingivalis* by newly developed gingipain inhibitors. *Mol. Pharmacol.* **2004**, *66*, 1599−1606.
(9) Slots, J.; Bragd, L.; Wikstrom, M.; Dahlen, G. The occurrence of *Actinobacillus actinomycetemcomitans*, *Bacteroides gingivalis* and *Bacteroides intermedius* in destructive periodontal disease in adults. *J. Clin. Periodontol.* **1986**, *13*, 570−577.
(10) Holt, S. C.; Ebersole, J.; Felton, J.; Brunsvold, M.; Kornman, K. S. Implantation of *Bacteroides gingivalis* in nonhuman primates initiates progression of periodontitis. *Science* **1988**, *239*, 55−57.
(11) Pike, R.; McGraw, W.; Potempa, J.; Travis, J. Lysine- and arginine-specific proteinases from *Porphyromonas gingivalis*. Isolation, characterization, and evidence for the existence of complexes with hemagglutinins. *J. Biol. Chem.* **1994**, *269*, 406−411.
(12) Potempa, J.; Mikolajczyk-Pawlinska, J.; Brassell, D.; Nelson, D.; Thogersen, I. B.; et al. Comparative properties of two cysteine proteinases (gingipains R), the products of two related but individual genes of *Porphyromonas gingivalis*. *J. Biol. Chem.* **1998**, *273*, 21648−21657.
(13) Nakayama, K.; Ratnayake, D. B.; Tsukuba, T.; Kadowaki, T.; Yamamoto, K.; et al. Haemoglobin receptor protein is intragenically encoded by the cysteine proteinase-encoding genes and the haemagglutinin-encoding gene of *Porphyromonas gingivalis*. *Mol. Microbiol.* **1998**, *27*, 51−61.
(14) Okamoto, K.; Nakayama, K.; Kadowaki, T.; Abe, N.; Ratnayake, D. B.; et al. Involvement of a lysine-specific cysteine proteinase in hemoglobin adsorption and heme accumulation by *Porphyromonas gingivalis*. *J. Biol. Chem.* **1998**, *273*, 21225−21231.

(15) Genco, C. A.; Potempa, J.; Mikolajczyk-Pawlinska, J.; Travis, J. Role of gingipains R in the pathogenesis of *Porphyromonas gingivalis*-mediated periodontal disease. *Clin. Infect. Dis.* **1999**, *28*, 456−465.
(16) Graves, D. T.; Jiang, Y.; Genco, C. Periodontal disease: Bacterial virulence factors, host response and impact on systemic health. *Curr. Opin. Infect. Dis.* **2000**, *13*, 227−232.
(17) Imamura, T. The role of gingipains in the pathogenesis of periodontal disease. *J. Periodontol.* **2003**, *74*, 111−118.
(18) Abe, N.; Kadowaki, T.; Okamoto, K.; Nakayama, K.; Ohishi, M.; et al. Biochemical and functional properties of lysine-specific cysteine proteinase (Lys-gingipain) as a virulence factor of *Porphyromonas gingivalis* in periodontal disease. *J. Biochem. (Tokyo)* **1998**, *123*, 305−312.
(19) Travis, J.; Potempa, J. Bacterial proteinases as targets for the development of second-generation antibiotics. *Biochim. Biophys. Acta* **2000**, *1477*, 35−50.
(20) Kadowaki, T.; Yamamoto, K. Suppression of virulence of *Porphyromonas gingivalis* by potent inhibitors specific for gingipains. *Curr. Protein Pept. Sci.* **2003**, *4*, 451−458.
(21) Curtis, M. A.; Kuramitsu, H. K.; Lantz, M.; Macrina, F. L.; Nakayama, K.; et al. Molecular genetics and nomenclature of proteases of *Porphyromonas gingivalis*. *J. Periodontal. Res.* **1999**, *34*, 464−472.
(22) Pavloff, N.; Potempa, J.; Pike, R. N.; Prochazka, V.; Kiefer, M. C.; et al. Molecular cloning and structural characterization of the Arg-gingipain proteinase of *Porphyromonas gingivalis*. Biosynthesis as a proteinase-adhesin polyprotein. *J. Biol. Chem.* **1995**, *270*, 1007−1010.
(23) Rangarajan, M.; Aduse-Opoku, J.; Slaney, J. M.; Young, K. A.; Curtis, M. A. The prpR1 and prR2 arginine-specific protease genes of *Porphyromonas gingivalis* W50 produce five biochemically distinct enzymes. *Mol. Microbiol.* **1997**, *23*, 955−965.
(24) Gusman, H.; Travis, J.; Helmerhorst, E. J.; Potempa, J.; Troxler, R. F.; et al. Salivary histatin 5 is an inhibitor of both host and bacterial enzymes implicated in periodontal disease. *Infect. Immun.* **2001**, *69*, 1402−1408.
(25) Snipas, S. J.; Stennicke, H. R.; Riedl, S.; Potempa, J.; Travis, J.; et al. Inhibition of distant caspase homologues by natural caspase inhibitors. *Biochem. J.* **2001**, *357*, 575−580.
(26) Kadowaki, T.; Kitano, S.; Baba, A.; Takii, R.; Hashimoto, M.; et al. Isolation and characterization of a novel and potent inhibitor of Arg-gingipain from *Streptomyces* sp. strain FA-70. *Biol. Chem.* **2003**, 384, 911−920.
(27) Imamura, T.; Matsushita, K.; Travis, J.; Potempa, J. Inhibition of trypsin-like cysteine proteinases (gingipains) from *Porphyromonas gingivalis* by tetracycline and its analogues. *Antimicrob. Agents Chemother.* **2001**, *45*, 2871−2876.
(28) Potempa, J.; Pike, R.; Travis, J. Titration and mapping of the active site of cysteine proteinases from *Porphyromonas gingivalis* (gingipains) using peptidyl chloromethanes. *Biol. Chem.* **1997**, *378*, 223−230.
(29) Curtis, M. A.; Aduse Opoku, J.; Rangarajan, M.; Gallagher, A.; Sterne, J. A.; et al. Attenuation of the virulence of *Porphyromonas gingivalis* by using a specific synthetic Kgp protease inhibitor. *Infect. Immun.* **2002**, *70*, 6968−6975.
(30) Ekici, O. D.; Gotz, M. G.; James, K. E.; Li, Z. Z.; Rukamp, B. J.; et al. Aza-peptide Michael acceptors: A new class of inhibitors specific for caspases and other clan CD cysteine proteases. *J. Med. Chem.* **2004**, *47*, 1889−1892.
(31) Krauser, J. A.; Potempa, J.; Travis, J.; Powers, J. C. Inhibition of arginine gingipains (RgpB and HRgpA) with benzamidine inhibitors: Zinc increases inhibitory potency. *Biol. Chem.* **2002**, *383*, 1193−1198.
(32) Otto, H. H.; Schirmeister, T. Cysteine proteases and their inhibitors. *Chem. Rev.* **1997**, *97*, 133−172.
(33) Leung, D.; Abbenante, G.; Fairlie, D. P. Protease inhibitors: Current status and future prospects. *J. Med. Chem.* **2000**, *43*, 305−341.
(34) Bohm, H. J. LUDI: Rule-based automatic design of new substituents for enzyme inhibitor leads. *J. Comput. Aided Mol. Des.* **1992**, *6*, 593−606.
(35) Bohm, H. J. A novel computational tool for automated structure-based drug design. *J. Mol. Recognit.* **1993**, *6*, 131−137.
(36) Berger, A.; Schechter, I. Mapping the active site of papain with the aid of peptide substrates and inhibitors. *Philos. Trans. R. Soc. London B Biol. Sci.* **1970**, *257*, 249−264.
(37) Sali, A.; Blundell, T. L. Comparative protein modelling by satisfaction of spatial restraints. *J. Mol. Biol.* **1993**, *234*.
(38) Eichinger, A.; Beisel, H. G.; Jacob, U.; Huber, R.; Medrano, F. J.; et al. Crystal structure of gingipain R: An Arg-specific bacterial cysteine proteinase with a caspase-like fold. *EMBO J.* **1999**, *18*, 5453−5462.
(39) Bohm, H. J. The development of a simple empirical scoring function to estimate the binding constant for a protein−ligand complex of known three-dimensional structure. *J. Comput. Aided Mol. Des.* **1994**, *8*, 243−256.
(40) *Ligand_Design 97 Molecular Modelling Program Package*; 97.0 ed.; Molecular Simulations Inc.: San Diego, CA.
(41) Steinmetzer, T.; Konishi, Y. Tripeptydyl pyridinium methyl ketones as potent active site inhibitors of thrombin. *Bioorg. Med. Chem. Lett.* **1996**, *6*, 1677−1682.
(42) Grembecka, J.; Mucha, A.; Cierpicki, T.; Kafarski, P. The most potent organophosphorus inhibitors of leucine aminopeptidase. Structure-based design, chemistry, and activity. *J. Med. Chem.* **2003**, *46*, 2641−2655.
(43) Dyguda, E.; Grembecka, J.; Sokalski, W. A.; Leszczynski, J. Origins of the activity of PAL and LAP enzyme inhibitors: Toward ab initio binding affinity prediction. *J. Am. Chem. Soc.* **2005**, *127*, 1658−1659.
(44) *Insight 97 Molecular Modelling Program Package*; 97.0 ed.; Molecular Simulations Inc.: San Diego, CA.
(45) *Discover, Molecular Modelling Program Package*; 97.0 ed.; Molecular Simulation: San Diego, CA.
(46) Steinmetzer, T.; Zhu, B. Y.; Konishi, Y. Potent bivalent thrombin inhibitors: Replacement of the scissile peptide bond at P(1)−P(1)′ with arginyl ketomethylene isosteres. *J. Med. Chem.* **1999**, *42*, 3109−3115.

JM0600141